Nucleic Acids Research, 2006, Vol. 34, No. 12 ***3409–3420***
doi:10.1093/nar/gkl393

Lac repressor hinge flexibility and DNA looping: single molecule kinetics by tethered particle motion

Francesco Vanzi[1,2,*], Chiara Broggio[1,3], Leonardo Sacconi[1] and Francesco Saverio Pavone[1,4]

[1]LENS—European Laboratory for Nonlinear Spectroscopy, University of Florence, Italy, [2]Department of Animal Biology and Genetics 'Leo Pardi', University of Florence, Italy, [3]Department of Physics, University of Trento, Italy and [4]Department of Physics, University of Florence, Italy

Received February 15, 2006; Revised April 13, 2006; Accepted May 9, 2006

ABSTRACT

The tethered particle motion (TPM) allows the direct detection of activity of a variety of biomolecules at the single molecule level. First pioneered for RNA polymerase, it has recently been applied also to other enzymes. In this work we employ TPM for a systematic investigation of the kinetics of DNA looping by wild-type Lac repressor (wt-LacI) and by hinge mutants Q60G and Q60 + 1. We implement a novel method for TPM data analysis to reliably measure the kinetics of loop formation and disruption and to quantify the effects of the protein hinge flexibility and of DNA loop strain on such kinetics. We demonstrate that the flexibility of the protein hinge has a profound effect on the lifetime of the looped state. Our measurements also show that the DNA bending energy plays a minor role on loop disruption kinetics, while a strong effect is seen on the kinetics of loop formation. These observations substantiate the growing number of theoretical studies aimed at characterizing the effects of DNA flexibility, tension and torsion on the kinetics of protein binding and dissociation, strengthening the idea that these mechanical factors *in vivo* may play an important role in the modulation of gene expression regulation.

INTRODUCTION

Since its first description, formulated more than 40 years ago (1), the Lac operon has represented a crucial system for understanding basic mechanisms of gene regulation and the response of living organisms to changes in the environment. Over the past decades, a wealth of information on the molecular structure and mechanisms of this system has been provided by genetics, biochemistry and structural biology, leading to a detailed picture of the genetic elements of the Lac operon, the atomic structure of the Lac repressor (LacI) and the kinetics and thermodynamics of interaction LacI–DNA [for a recent review see (2)].

One fundamental aspect, emerging from several studies, is that LacI can bind simultaneously to two operators on the DNA (normally the primary operator and a second sequence, termed a pseudooperator), forming a loop in the intervening sequence. The property of looping DNA is common to other regulatory proteins and even restriction enzymes [for a review on DNA looping see (3)]. In the Lac operon, the pseudooperators are positioned at 92 and 401 bp from the primary operator (4,5), leading to the possibility of formation of DNA loops of corresponding lengths. Depending on the concentration of accessory proteins capable of inducing bends in the DNA molecule and effectively reducing its persistence length (6), the formation of such loops can imply significant bending energies (of the order of several k_BT). The effect of the DNA bending energy on the kinetics of protein binding and loop formation, thus represents a potentially important means for the modulation of gene expression regulation at a global or local level on the cell genome. *In vitro* the role of DNA flexibility on ligase-catalyzed cyclization has been extensively characterized (7–10) and several theoretical studies have been produced to interpret those results (11,12). From these considerations, a picture is emerging in which DNA is not just simply a passive substrate of regulatory and processing enzymes, but indeed an active player with dynamic physical properties capable of influencing the activity of all DNA-binding proteins. On the other hand, it is then fundamental to gain understanding of the mechanics of DNA-binding proteins, with particular regard to the interplay between their flexibility and the dependence of their kinetics on the DNA physical properties.

Recently, quantitative theories have been formulated on the effects of force on protein–DNA interaction (13–15), leading to the interesting hypothesis that force may play a significant role on gene expression regulation *in vivo*.

*To whom correspondence should be addressed at LENS—Via Nello Carrara 1, 50019 Sesto Fiorentino (FI)—Italy. Tel: +39 055 457 2476; Fax: +39 055 457 2451; Email: fvanzi@lens.unifi.it

Based on these considerations, it is very interesting to investigate the role of DNA and protein mechanics on the mechanism of regulation of gene expression in the Lac operon.

Direct observation of DNA looping by LacI was first provided by electron microscopy (16). Measurements *in vivo* (17,18) and *in vitro* (19) have provided crucial information on the effects of operators spacing and phasing on the stability of the LacI-induced loop. However, a fundamental aspect of repression through DNA looping is represented by the kinetics of formation and disruption of the DNA loop, which are not directly measurable with electron microscopy or biochemical binding assays. With the tethered particle motion (TPM) method, Finzi and Gelles (20) first demonstrated the possibility of observing directly the formation and disruption of a LacI-induced loop in a single DNA molecule and of measuring the kinetics of these processes. Figure 1 shows a scheme of the TPM system: a DNA molecule containing two appropriately spaced operators is anchored with one end to the surface of a microscope coverslip, while the other end is tagged with a microsphere. The range of Brownian diffusion of the microsphere is limited by the DNA tether. Upon binding of LacI simultaneously to both operators, the tether is effectively shortened, leading to a measurable reduction in the range of diffusion of the microsphere.

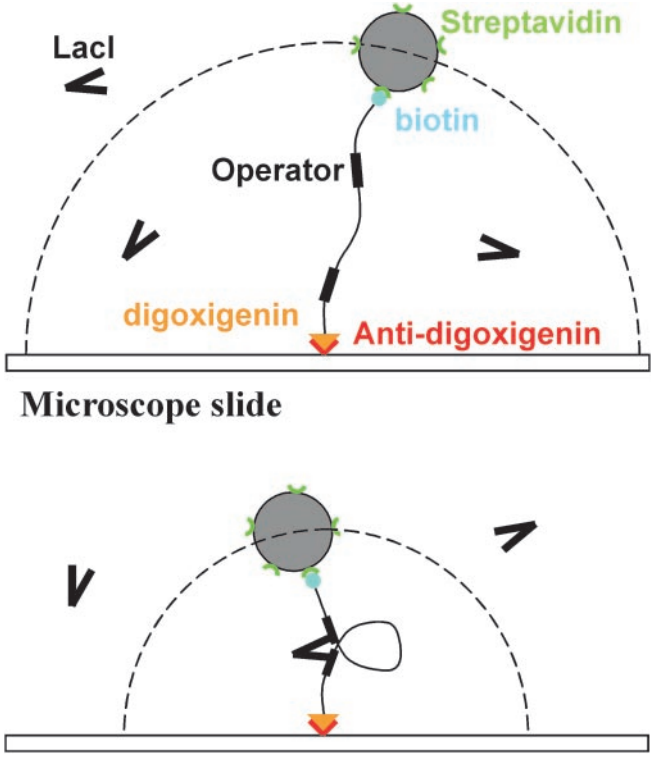

Figure 1. The TPM experiment. The DNA molecule is shown in black, with the two operators highlighted by the black boxes. The Lac repressor tetramer (LacI) is schematically drawn as a V-shaped molecule. The microsphere is shown in gray and the range of diffusion allowed to the sphere by the DNA tether is shown as a dashed line. The upper panel shows unlooped DNA, the lower panel shows the same molecule looped by the binding of a Lac repressor tetramer to the two operators. The drawing is not to scale.

TPM measurements of a 305 bp long LacI-induced loop indicated that this state is characterized by mono-exponentially distributed durations and does not seem significantly influenced by the bending energy stored in the DNA loop (20). The lifetime distribution of the unlooped state, on the other hand, exhibited a more complex shape (at least bi-exponential), as expected of a species which could be due to a manifold of biochemical states (e.g. both operators vacant, both operators occupied by a LacI tetramer, one operator occupied by LacI tetramer or dimer and the other vacant, and so on). Therefore, a more detailed analysis of such distribution (and, thus, of the possible effects of bending and twisting energy on the rate of loop formation) was not attempted.

In this work we present results obtained applying the TPM technique to the study of wild-type Lac repressor (wt-LacI) at different concentrations, as well as to two mutants of the hinge region: Q60G and Q60 + 1 (21). A full characterization of the TPM data reveals that, due to the limited signal-to-noise ratio of this technique, the measurement of kinetic parameters, such as the average lifetime of the looped and unlooped state, is critically affected by the extent of filtering of the data. We elaborated a novel mathematical method for analyzing TPM data and obtained unbiased estimates of the kinetics of looping and unlooping. This provides the basis for obtaining, from this simple single molecule technique, a much more detailed picture of the LacI–DNA interaction mechanisms, including the first experimental evidence for the role of LacI hinge flexibility and DNA bending energy on the kinetics of the process. Using wild-type LacI, we demonstrate that the rate of disruption of the loop is barely affected by the DNA bending energy, as originally suggested also by Finzi and Gelles (20). On the other hand, our measurements clearly indicate that the rate of formation of the loop is strongly affected by the energetics of DNA bending. To follow up on this well-expected dependence of the rate of loop formation on DNA bending energetics, we investigated also the role of the flexibility of the protein on this process. Particularly interesting, in this regard, is the flexibility of the hinge region of LacI, which connects the core of the protein with the DNA-binding head. The variations of flexibility and geometry of the hinge region in the two mutations studied are associated with very significant changes in the durations of the looped and, to a lesser extent, unlooped states measured by TPM, demonstrating the interplay between DNA and protein flexibility in the modulation of the rates of formation and breakdown of the regulatory loop in the lac operon. Interestingly, the flexibility of the hinge, while drastically changing the looping/unlooping dynamics does not significantly alter the dependence of those dynamics on the DNA strain.

These measurements indicate that the Lac operon is a genetic system potentially very sensitive to the mechanics of DNA and of Lac repressor itself.

MATERIALS AND METHODS

Preparation of proteins and DNA

Lac repressor (both wild-type and mutants) was overexpressed in BLIM cells (22) and purified according to Chen

and Matthews (23). The DNA construct used in TPM experiments was synthesized by PCR similarly to the method described by Finzi and Gelles (20). Briefly, the pRW490 plasmid (19), containing two primary operators (with sequence 5′-TGTTGTGTGGAATTGTGAGCGGATAACAAT-TTCACACAGG-3′) spaced 305 bp apart, was used as template in a PCR (201223, Qiagen, Germany) employing the following primers (MWG-Biotech AG, Germany): 5′-Biotin-AGATCCAGTTCGATGT-3′; 5′-Digoxigenin-ATAGTGGCTCCAAGTAGC-3′.

The PCR product (purified using 28104, Qiagen, Germany) is a 1302 bp molecule labeled with biotin at one end and with digoxigenin at the other end (see Figure 1).

A flow chamber (with a volume of ~20 µl) was constructed between a microscope slide and a coverslip kept at a distance of ~60 µm by double-sided tape. Strips of silicon grease were deposited on the inner side of the tape to provide lateral sealing and avoid contact of the solution with the tape itself. The microscope slides were previously cleaned in an ultrasonic bath in ethanol for 5 min. The coverslips were cleaned further by a 10 min treatment with reactive ion plasma in a radio-frequency plasma cleaner (PDC-002, Harrick Inc., NY).

Buffers and sample preparation for TPM

Unless otherwise specified, all chemicals and reagents were purchased from Sigma–Aldrich. The sample was prepared as follows. All steps were performed at room temperature; long incubations were conducted in a water-saturated container to avoid evaporation of the sample. A solution containing 20 µg/ml anti-digoxigenin (1333089, Roche, IN) in phosphate-buffered saline (PBS) buffer [2.7 mM KCl, 137 mM NaCl, 5.4 mM Na_2HPO_4 and 1.8 mM KH_2PO_4 (pH 7.4)] was introduced into the flow chamber and incubated for 20 min to insure optimal surface coating. The excess antibody was then removed by washing the chamber 5–7 times with 80 µl of LBB buffer [10 mM Tris–HCl (pH 7.4), 200 mM KCl, 0.1 mM EDTA, 5% (v/v) dimethyl sulfoxide (DMSO), 0.2 mM DTT, 0.1 mg/ml α-casein]. The DNA sample (80 µl at a concentration of ~20 ng/ml in LBB buffer: this DNA concentration was chosen to maximize single DNA tethers as described below) was then introduced in the chamber and incubated for 1 h. Unbound DNA was removed by washing with 7 × 50 µl LBB^- buffer (LBB lacking DTT and DMSO). Streptavidin-coated polystyrene microspheres (diameter 440 nm, Indicia Biotechnology, France) in LBB^- buffer were then introduced in the flow chamber and incubated for 30 min. Unbound microspheres were finally removed with 5 × 50 µl washes of LBB buffer supplemented with Lac repressor at a tetramer concentration of 4, 20 or 100 pM, depending on the experiment. The flow chamber was then sealed with silicon grease to allow prolonged observation at the microscope (each slide could be observed for several hours without detectable loss in activity of LacI).

Data collection and analysis

The slide was mounted on an inverted microscope (Eclipse TE300, Nikon, Japan), images of a region of interest containing the microsphere chosen were acquired at a frequency of 25 Hz with a video camera (C3077-71, Hamamatsu, Japan) and digitized with an A/D converter (IMAQ PCI-1408, National Instruments, TX). The software for instrumentation control, data acquisition and data processing was written in Labview (v. 6.0, National Instruments, TX). Microspheres were chosen for recording based on the range of mobility exhibited; each microsphere was normally monitored for ~1 h.

The position of the microsphere in the sample plane (x-y plane) was monitored in real-time during the experiment using a centroid algorithm (24,25): each video frame was deinterlaced and calculation of the centroid was performed separately, after background subtraction, on the even and odd lines of the image, to obtain measurements of the bead's position with a frequency of 50 Hz. The average radius of mobility of the microsphere was calculated in real-time and charted, during the experiment, at the desired frequency. The x and y coordinates of the microsphere, determined at a frequency of 50 Hz, were also stored for subsequent analysis as described below. Symmetry of the distribution of centroid positions in the x-y plane was used as diagnostic to insure that the microsphere would not be tethered by multiple DNA molecules or be perturbed in its diffusive motion by surface irregularities (25,26). Additionally, the DNA dilution adopted for all experiments had been previously optimized for a relatively high yield of tethered microspheres (density of about 1 tethered microsphere in each microscope field of 34 × 26 μm^2) with a negligible probability of multiple DNA molecules bound to the same microsphere.

At the end of the experiment, data were analyzed as follows. Slow apparatus fluctuations and drift in stage position were removed from the $x(t)$ and $y(t)$ recordings by filtering the data with a Butterworth high-pass filter (cutoff frequency of 0.1 Hz). From the filtered data, $R(t)$ was then calculated as $\sqrt{[x(t)]^2+[y(t)]^2}$ and a running average $\langle R(t)\rangle$ was calculated by filtering the $R(t)$ trace with a Gaussian filter (27). For each microsphere a set of four $\langle R(t)\rangle$ traces was calculated using Gaussian filters with cutoff frequencies of 0.133, 0.066, 0.044 and 0.033 Hz, corresponding to standard deviations of the filter's impulse response of 1, 2, 3 and 4 s, respectively. The left panels of Figures 2 and 3 show examples of $\langle R(t)\rangle$ traces obtained with a filter cutoff frequency of 0.066 Hz.

Dwell-times were extracted from each $\langle R(t)\rangle$ recording using a half-amplitude threshold method (27): the $\langle R(t)\rangle$ distribution (the right panels of Figures 2 and 3 show some examples) was fitted with a double Gaussian: $A_1 \exp[-(x-xc_1)^2/2\sigma_1^2] + A_2 \exp[-(x-xc_2)^2/2\sigma_2^2]$. For each recording, the threshold was set half way between the peaks of the two fitted Gaussian curves.

A first semi-quantitative analysis of dwell-times was elaborated following a method analogous to that described by Finzi and Gelles (20), which is based on the choice of a single filter: the $R(t)$ data were filtered with cutoff frequency of 0.033 Hz, corresponding to a filter dead time (T_d) of 5.4 s. The transitions giving raise to events shorter than T_d were ignored (20,28) and the resulting dwell-time distributions were analyzed to produce the durations histograms, reporting only the events with durations longer than $2T_d$ (20,27).

Then, a full characterization of the analysis method was conducted using filters with different cutoff frequencies

(0.133, 0.066, 0.044 and 0.033 Hz) as mentioned above. From the measured distributions of dwell-times, the average lifetime of the looped (τ_{Lm}) and the unlooped (τ_{Um}) states were calculated for each experimental condition studied. In the results section we will show that these measured parameters strongly depend on the choice of filter operated. Thus, we developed a set of mathematical corrections aimed at obtaining, from the TPM measurements, a reliable estimate of the average duration of the looped and unlooped state in the DNA molecule, regardless of the choice of filter and the effects of residual noise in the measurements (see Supplementary Data). For this analysis, dwell-times were measured without imposing any cutoff in duration, since filter's limited time resolution (27) and false events due to noise are taken into account in our analysis method.

The full description of the derivation of our novel method will be published elsewhere; here we provide the mathematical expressions applied to the experimental results presented in this paper for wt-LacI at different concentrations and the Q60G and Q60 + 1 mutants. A description of the corrections used in this work and a demonstration of the validity of this method, based on numerical simulations, is reported in the Supplementary Data.

RESULTS

The TPM measurements were performed either with wt-LacI at different concentrations (4, 20 and 100 pM) or with Lac repressor mutants of the hinge region Q60G and Q60 + 1 (21) at 100 pM concentration. Figure 2a, c and e shows typical TPM recordings obtained with wt-LacI at 100 pM, 20 pM and 4 pM, respectively. Figure 3a and c shows typical TPM recordings obtained with the mutants Q60G and Q60 + 1 both at a concentration of 100 pM. In all traces an alternation between two distinct levels of microsphere mobility can be noticed, as evidenced also by the histograms of $\langle R(t)\rangle$ reported in the right panels of Figures 2 and 3. A certain extent of bead-to-bead hetrerogeneity in the values of $\langle R\rangle$ in looped and unlooped state can be observed from the histograms in the right panels of the figures, presumably due to possible small effects of long-range surface–microsphere (or surface–DNA) interactions on the diffusion of the microsphere. The difference in $\langle R\rangle$ between the two states (ϕ) is, however, very consistent throughout all measurements, as quantified in the Supplementary Table. This result suggests that the observed transitions between the lower and higher state of microsphere mobility measured in TPM report the switching of the system between two well-defined geometries. The lack of a dispersed population of looped configurations confirms that nonspecific binding of LacI to DNA does not play a significant role in the TPM measurements, as also expected based on the equilibrium association constants for specific and nonspecific sequences (there is a difference of about seven orders of magnitude between the two equilibrium constants and only about three orders of magnitude in the relative concentrations between operator target and nonspecific sequences in our 1300 bp construct).

As reported also by Finzi and Gelles (20), addition of isopropyl-β-D-thiogalactopyranoside (IPTG) at a concentration of 1 mM completely abolished the alternation between two states, determining one constant level corresponding to the larger mobility of the microsphere. This control was performed both for wt-LacI and for the two mutants (data not shown). Thus, we attribute the lower and higher microsphere mobility state to the system in a looped and unlooped configuration, respectively, as shown in Figure 1.

The qualitative differences among the traces shown in Figures 2 and 3 are evident upon inspection: the decrease in concentration of wt-LacI determines a significant shortening of the unloop durations, whereas the loop state is much less affected. In fact, at the lower concentrations most unloop states appear as short spikes in the TPM recording, while a few events still retain a duration of few hundred seconds. At a LacI concentration of 4 pM, the average rate of association of free LacI in solution to one operator is $\sim 5 \cdot 10^{-3}$ s^{-1}; in these conditions, the increase of duration in the longer unloop states as a function of decreasing LacI concentration is, however, difficult to quantify experimentally, since it would require very long recordings. In general, mechanical drifts and fluctuations of the apparatus limit the duration of experimental TPM recordings to 1–1.5 h, leading to loss or truncation of a significant fraction of the events lasting several hundreds seconds.

On the other hand, the two mutants display, with respect to wt-LacI at the same concentration, variations that correlate with the measured changes of K_D (21): Q60G (characterized by a K_D about three times smaller than wt-LacI) displays much longer durations for the loop state; whereas Q60 + 1 (characterized by a K_D about three times larger than wt-LacI) displays a much more dynamic behavior with very short loop and unloop states. These results demonstrate that hinge flexibility has a profound effect on the looping/unlooping dynamics of LacI.

A first semi-quantitative analysis of the data, with a method analogous to that described by Finzi and Gelles (20), yields the results shown in Figures 4 and 5. The lack of dependence of τ_{Lm} on wt-LacI concentration, together with the mono-exponential distribution of the dwell-times of the TPM looped state (Figures 4 and 5, left panels) indicate that this TPM state has a 1:1 correspondence to the biochemical LacI–DNA complex in a looped configuration (see Discussion). The multi-exponential nature of the lifetime distribution for the unlooped state (Figures 4 and 5, right panels, in which the fit with a double-exponential is shown), on the other hand, indicates that the TPM state characterized by the larger microsphere mobility corresponds to a variety of possible biochemical states, in principle up to nine (20,29). However, at all the concentrations used in these experiments, the fraction of Lac repressor present in solution as a dimer is negligible (30,31), so that the scheme of biochemical states corresponding to the measured TPM states simplifies as shown in Figure 6. In this scheme, the TPM unloop state corresponds to a sum of the O-O, O-OR and RO-OR biochemical states.

Based on these considerations, we define the relationship $2k_d\alpha = (\tau_L)^{-1}$, in which the disruption of the loop occurs at a rate which is twice the rate of dissociation of each repressor/operator interface (k_d), modified by a factor α incorporating the possible effects of DNA strain.

In the scheme of Figure 6, J_m represents the effective concentration of the vacant operator (32) for the association to the RO complex on the same DNA molecule. In the TPM

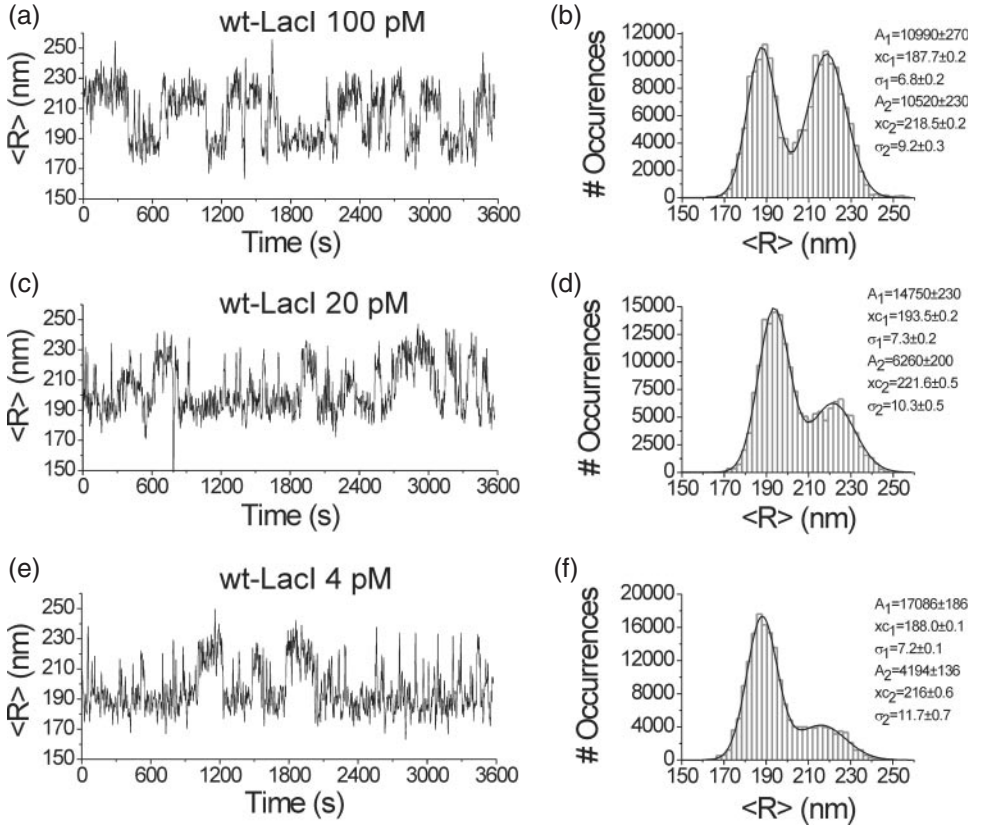

Figure 2. Examples of TPM experimental recordings obtained with wild-type LacI. The left panels show time courses of the average radius of microsphere mobility, $\langle R(t) \rangle$ (calculated as described in the Materials and Methods section, choosing a Gaussian filter with cutoff frequency of 0.066 Hz) obtained with LacI at a concentration of 100 pM (**a**), 20 pM (**c**), and 4 pM (**e**). The right panels show the distributions of $\langle R(t) \rangle$ corresponding to each of the recordings shown on the left. The lines represent the best fit of the sum of two Gaussians (see Materials and Methods) to the histogram. The fitted parameters are shown in the insets.

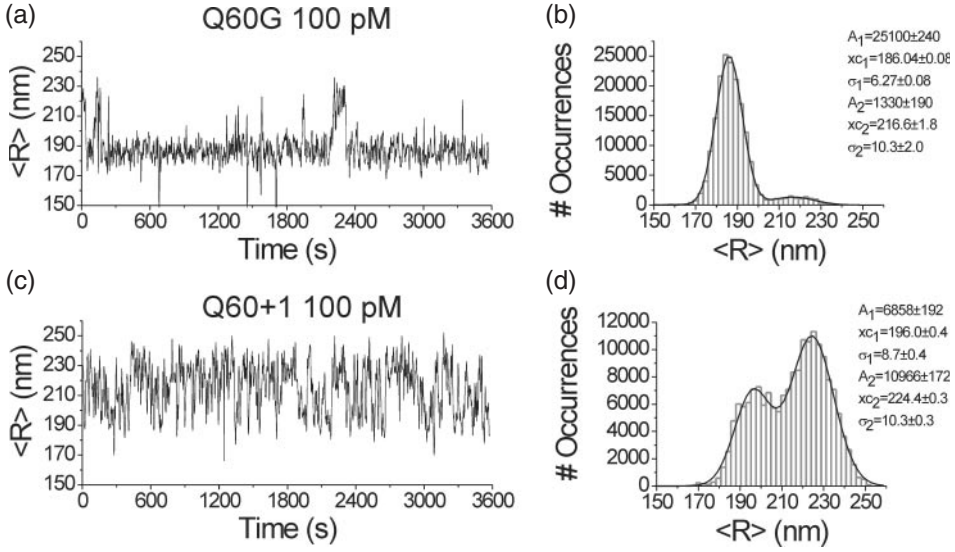

Figure 3. Examples of TPM experimental recordings obtained with LacI mutants Q60G and Q60 + 1. The left panels show time courses of the average radius of mobility, $\langle R(t) \rangle$ (calculated as in Figure 2), obtained with Q60G (**a**) and Q60 + 1 (**c**) at a concentration of 100 pM. Histograms (shown on the right) are fitted with two Gaussians as described in Figure 2.

experiment this parameter can be modified by the presence of the microsphere, as discussed in much more detail below.

The comparison of the lifetime of the looped state determined on the DNA molecule by wt-LacI (at 100 pM concentration, Figure 4a) and by the hinge mutants (Figure 5a and c) shows that the kinetics of rupture of the loop mirror quantitatively the values measured for K_D (21), as mentioned above. In the absence of experimental

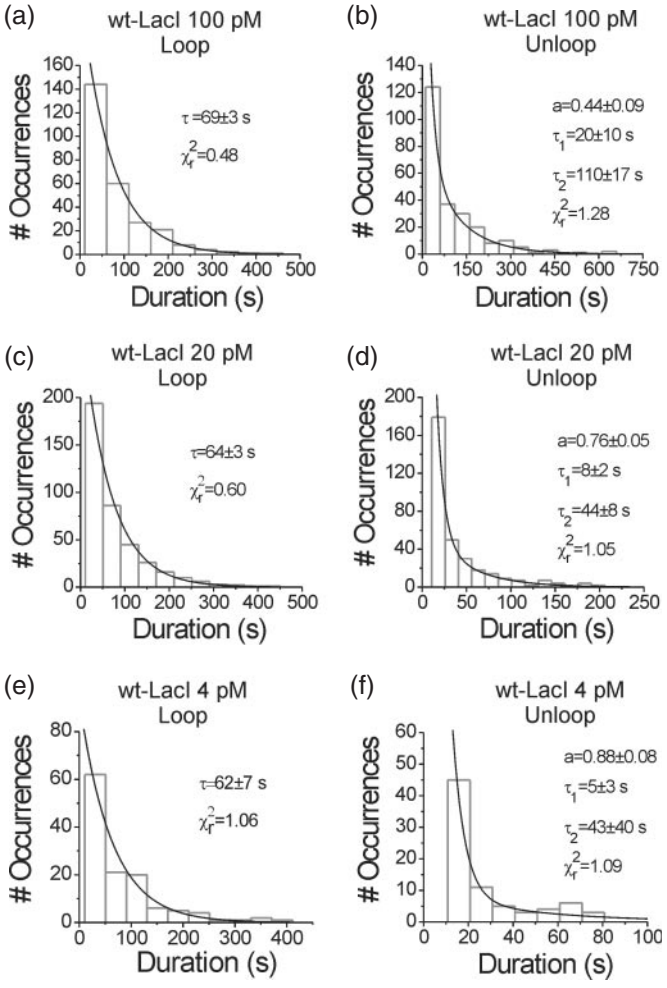

Figure 4. Distributions of dwell-times of wild-type LacI. The histograms are distributions of the loop (left) and unloop (right) dwell-times measured on TPM recordings obtained with wild-type LacI at concentrations of 100 pM (**a**: loop; **b**: unloop), 20 pM (**c**: loop; **d**: unloop) and 4 pM (**e**: loop; **f**: unloop). The dwell-times were measured after filtering the $\langle R(t)\rangle$ data, as described in text, with a Gaussian filter with a cutoff frequency of 0.033 Hz, characterized by a dead time of 5.4 s. Only events with durations longer than twice the dead time are plotted. The lines in the left panels represent fit to the data using a mono-exponential function $N(t) = (wN_{tot}/\tau)exp[-(t - t_0)/\tau]$, where N_{tot} is the total number of events observed, w is the histogram bin width, and t_0 is the shortest plotted duration (10.8 s). The insets report the value of the fitted parameter τ and the reduced χ^2. The lines in the right panels represent fit to the data using a double-exponential function $N(t)=wN_{tot}[(a/\tau_1)\exp(-t/\tau_1)+((1-a)/\tau_2)\exp(-t/\tau_2)]/[a\exp(-t_0/\tau_1)+(1-a)\exp(-t_0/\tau_2)]$.

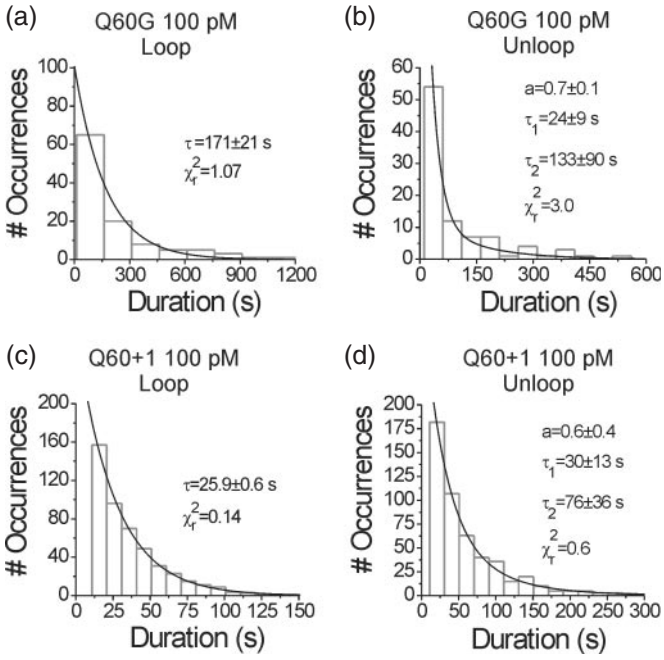

Figure 5. Distributions of dwell-times of the LacI mutants Q60G and Q60 + 1. The histograms are distributions of the loop (left) and unloop (right) dwell-times measured on TPM recordings obtained with Q60G (**a**: loop; **b**: unloop) and Q60 + 1 (**c**: loop; **d**: unloop) at a concentration of 100 pM. The histogram and the fit in the left panels were obtained as described in Figure 4.

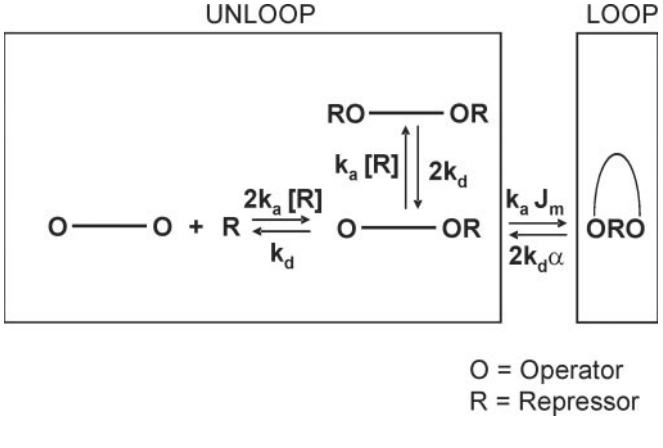

Figure 6. Scheme of the biochemical states corresponding to the loop and unloop states as measured with TPM. O and R represent the operator sequence and the Lac repressor tetramer, respectively. k_a and k_d are the association and dissociation rate constants of LacI for a single operator. J_m and α are defined in the text. The segment between the two operators represents the intervening (305 bp long) DNA sequence.

biochemical measurements of the association and dissociation rate constants for these mutants, our single molecule results indicate that the variations induced in the equilibrium constant K_D by the mutations studied are largely due to variations in the dissociation rate constant k_d. These results demonstrate that the flexibility of the hinge region of LacI plays a fundamental role in determining the lifetime of the looped state and, thus, the efficiency of repression. The interplay between protein flexibility and DNA strain will be discussed further below.

As mentioned in the methods section, the quantitative kinetic interpretation of the TPM data requires filtering and subsequent careful analysis to take into account the effects of the filter itself on the measured variables. This is clearly demonstrated in Figure 7: the figure shows the trends of measured τ_{Lm} and τ_{Um} as a function of the filter's dead time (T_d) for the five experimental conditions tested (the three concentrations of wt-LacI and the two mutants at 100 pM concentration). It is very clear that, in all cases, the measured kinetics of looping and unlooping are biased by the filter and there is no obvious choice of an optimal filter. Before undertaking a complete analysis of this problem, however, it is worth considering some important and general

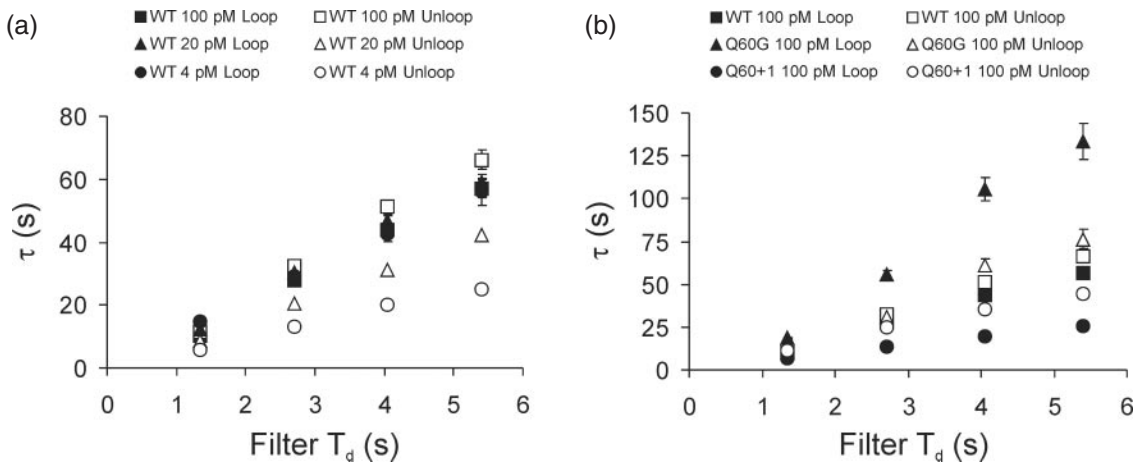

Figure 7. Choice of filter and measured looped and unlooped lifetimes. The measured average lifetimes are reported as a function of the filter dead time (T_d). (**a**): the average loop (filled symbols) and unloop lifetimes (empty symbols) are shown for wt-LacI at 100 pM (squares), 20 pM (triangles) and 4 pM (circles). (**b**): the average loop (filled symbols) and unloop lifetimes (empty symbols) are shown for wild-type LacI (squares), Q60G (triangles) and Q60 + 1 (circles), all at a concentration of 100 pM.

observations that can be obtained from the data analysis conducted thus far. Figure 7a shows the lifetimes measured at the three different concentrations of wt-LacI: for all choices of filter, τ_{Lm} (filled symbols) does not significantly depend on LacI concentration, whereas τ_{Um} (empty symbols) decreases with decreasing LacI concentration.

Considering that the TPM unloop state is the sum of O-O, O-OR and RO-OR (as discussed above), and applying the conditions of steady-state for each of the reactions in the biochemical scheme of Figure 6, the equilibrium partition between the two TPM states (L and U) is described by the following relationship:

$$\frac{L}{U} = \frac{J_m}{\alpha} \cdot \frac{[LacR] \cdot k_a^2}{(k_d + [LacR] \cdot k_a)^2} \qquad \mathbf{1}$$

As reference values for k_d and k_a of wt-LacI we use those measured by Hsieh *et al*. (19) for the plasmid pLA322: $k_d = 6.1 \cdot 10^{-3}$ s^{-1}; $k_a = 6.2 \cdot 10^8$ M^{-1} s^{-1}. The occupancies L and U of the loop and unloop states, respectively, can be determined from our single molecule experiments: Figure 2 (right panels) shows the histograms of the distributions of $\langle R(t) \rangle$ calculated from typical TPM recordings (left panels) obtained at each wt-LacI concentration studied. These distributions are well fit by a double Gaussian (shown in the figure by the black line): the ratio of the areas under the two peaks (calculated as $A_1\sigma_1/A_2\sigma_2$) provides a measurement of L/U. Based on the measurements performed at 4, 20 and 100 pM wt-LacI, we obtain, respectively, L/U values of 2.4 ± 0.2 (n = 6), 1.7 ± 0.3 (n = 23) and 0.80 ± 0.08 (n = 17), where the numbers reported are mean ± stderr and n indicates the number of experimental recordings used in the statistics (each recording corresponds to a different microsphere). Applying Equation 1 to each of these measurements we obtain, respectively, the following estimates for the ratio J_m/α: (1.1 ± 0.2), (0.7 ± 0.2) and (1.0 ± 0.1) $\cdot 10^{-10}$ M, which are in excellent agreement with each other within the experimental error. The values reported were obtained considering experimental traces filtered with a Gaussian filter with a T_d of 2.7 s. However, the values measured for the ratio L/U (and, thus, the estimates of J_m/α) do not depend on the choice of the filter (data not shown). In fact, threshold-crossing is clearly influenced by the extent of filtering of the data (as demonstrated in Figure 7), whereas the areas under each Gaussian peak represent the total time spent by the system in the looped and unlooped state. False threshold-crossings (due to noise) or missed threshold-crossings (due to limited time resolution of the filter) have negligible effects on the total time the system spends in each state.

The L/U ratio was measured also for the TPM recordings performed using Q60G and Q60 + 1 at 100 pM concentration (with examples of experimental traces shown in Figure 3), yielding, respectively values of 2.9 ± 0.9 (n = 15) and 0.46 ± 0.03 (n = 16). Assuming that the changes measured in K_D for these two mutants (21) are to be attributed mostly to variations in k_d, the J_m/α ratios obtained applying Equation 1 to these measurements are (3.2 ± 1.0) and (0.9 ± 0.1) $\cdot 10^{-10}$ M for Q60G and Q60 + 1, respectively. In conclusion, from these measurements, the J_m/α ratio results $\approx 10^{-10}$ M, regardless of protein concentration and hinge flexibility.

The application of our new analysis method (see Supplementary Data) to our TPM data allows a direct measurement of the values of J_m and α. Table 1 reports the lifetimes measured for the looped and unlooped states at the three different wt-LacI concentrations tested, as well as the corrected values obtained for τ_L, α and J_m.

From the results in Table 1 it can be noticed that, within experimental errors, α has a value comprised between 1 and 2, implying small effects (if any) of the DNA bending energy on the stability of the looped structure. J_m, on the other hand, has a value which is much lower than those measured by ligase-catalyzed cyclization of DNA segments of corresponding lengths (8). The values of α and J_m measured at 4 pM are somewhat systematically larger than those measured at 20 and 100 pM; in this regard, however, it should be noticed that the measurements at 4 pM are more subject to a possible bias in the TPM system. The most likely source of bias is due to an intrinsic limit of the TPM measurement: at the lowest LacI concentrations,

Table 1. Measured and corrected kinetic parameters of looping and unlooping by wild-type Lac repressor

	T_d (s)	T_r (N_r)	N_{Lm}	τ_{Lm} (s)	N_{Um}	τ_{Um} (s)	τ_L corr. (s)	α	J_m (10^{-10} M)
100 pM	1.35	588 (13)	1647	10.2 ± 0.3	1642	11.2 ± 0.3	52 ± 26	1.6 ± 0.8	1.5 ± 0.7
	2.70	750 (17)	729	29.0 ± 1.1	725	32.9 ± 1.2	61 ± 13	1.3 ± 0.3	1.3 ± 0.3
	4.05	765 (17)	480	43.5 ± 2.0	476	52.6 ± 2.4	54 ± 9	1.5 ± 0.3	1.4 ± 0.3
	5.40	783 (18)	377	57.4 ± 2.9	372	68.1 ± 3.5	54 ± 8	1.5 ± 0.3	1.4 ± 0.2
20 pM	1.35	1003 (19)	2852	12.3 ± 0.2	2851	8.8 ± 0.2	38 ± 8	2.2 ± 0.5	1.1 ± 0.2
	2.70	1155 (23)	1354	30.5 ± 0.8	1358	20.7 ± 0.6	41 ± 10	2.0 ± 0.5	1.1 ± 0.5
	4.05	998 (20)	767	46.6 ± 1.7	771	31.2 ± 1.1	48 ± 4	1.7 ± 0.2	1.0 ± 0.1
	5.40	904 (18)	534	59.1 ± 2.6	538	42.1 ± 1.8	54 ± 5	1.5 ± 0.2	0.8 ± 0.1
4 pM	1.35	132 (3)	367	16.1 ± 0.8	369	5.5 ± 0.3	31 ± 8	2.6 ± 0.7	3.6 ± 0.9
	2.70	277 (6)	339	35.6 ± 1.9	342	13.3 ± 0.7	31 ± 4	2.6 ± 0.5	3.0 ± 0.4
	4.05	275 (6)	236	50.9 ± 3.3	239	18.8 ± 1.2	31 ± 4	2.6 ± 0.5	2.9 ± 0.4
	5.40	272 (6)	170	70.9 ± 5.4	175	24.4 ± 1.9	39 ± 6	2.1 ± 0.4	2.5 ± 0.4

The parameters reported are defined in the text. T_r is the total recording time (in minutes); N_r is the number of microspheres used for the statistics.

Table 2. Measured and corrected kinetic parameters of looping and unlooping by Lac repressor mutants Q60G and Q60 + 1

	T_d (s)	T_r (N_r)	N_{Lm}	τ_{Lm} (s)	N_{Um}	τ_{Um} (s)	τ_L corr. (s)	α	J_m (10^{-10} M)
Q60G	1.35	684 (14)	1409	18.7 ± 0.5	1413	10.4 ± 0.3	n.d.	n.d.	n.d.
	2.70	687 (15)	476	55.5 ± 2.5	480	30.8 ± 1.4	202 ± 132	1.2 ± 0.8	2.3 ± 1.4
	4.05	633 (15)	227	105.5 ± 7.0	230	51.2 ± 2.2	280 ± 162	0.9 ± 0.5	1.6 ± 0.9
	5.40	571 (14)	162	133.3 ± 10.5	166	76.4 ± 5.9	98 ± 90	2.5 ± 2.3	4.5 ± 3.9
Q60+1	1.35	722 (13)	2393	6.6 ± 0.1	2390	11.5 ± 0.2	16 ± 3	1.4 ± 0.3	1.0 ± 0.2
	2.70	839 (16)	1295	13.8 ± 0.4	1291	20.7 ± 0.6	15 ± 1	1.5 ± 0.2	1.1 ± 0.1
	4.05	829 (16)	896	19.9 ± 0.7	894	35.7 ± 1.2	16 ± 1	1.4 ± 0.2	1.2 ± 0.1
	5.40	823 (16)	705	25.9 ± 1.0	705	44.1 ± 1.7	18 ± 1	1.2 ± 0.1	1.2 ± 0.1

n.d. indicates that the numerical minimization algorithm employed in the correction method (see Supplementary Data) did not converge to a stable solution. T_r is the total recording time (in minutes); N_r is the number of microspheres used for the statistics.

the unloop events are represented (as shown in the example of Figure 2e) by trains of short spike-like events (due to the O-OR state), interrupted by longer unloop events (due to the O-O state), which have durations of several hundreds seconds. Due to the limited recording time in TPM (determined by mechanical fluctuations in the system and a certain amount of possible protein denaturation), a significant fraction of the latter events would be truncated or lost altogether, leading to a systematic underestimation of τ_U, and thus to the observed bias in the results. This type of bias is not measured by the uncertainties attributed to the measured parameters, since these stem from the experimental determination of the standard error on the measured dwell-times and cannot incorporate a possible systematic loss of the longer events. Furthermore, in the Supplementary Data it is shown that, in combination with the limitations just mentioned about the experimental TPM method, also the correction method is very reliable at 20 and 100 pM, but somewhat less reliable for measurements at 4 pM. For these reasons, while the qualitative behavior of the system at 4 pM concentration of LacI is interesting as a further element of characterization of the biochemistry underlying the TPM experiment, the quantitative conclusions drawn from experiments at the two higher concentrations must be considered much more reliable.

The J_m/α ratios that can be calculated using the values of J_m and α obtained from the kinetic analysis are all of the order of 10^{-10} M, in agreement with the ratios estimated directly from the L/U TPM occupancies.

Table 2 reports the lifetimes measured for the looped and unlooped states in the Q60G and Q60 + 1 mutants, as well as the corrected values obtained for τ_L, α and J_m.

The values reported for corrected τ_L, α and J_m were obtained applying our correction method to the experimentally determined values of N_U, N_L, τ_{Um}, τ_{Lm} and assuming that the changes of K_D measured in these mutants with respect to wt-LacI are due largely to changes in k_d. So, k_a was taken constant at $6.2 \cdot 10^8$ M^{-1} s^{-1}, while k_d was calculated at $2.03 \cdot 10^{-3}$ s^{-1} for Q60G and $2.29 \cdot 10^{-2}$ s^{-1} for Q60 + 1, based on the K_D values reported by Falcon and Matthews (21).

The values obtained for α and J_m are not significantly different from those obtained with wild-type LacI. It can be noticed that in the case of the Q60G mutant, the fluctuations in the reported values (along with their errors) are larger than in the other cases. This is due to the fact that the measurement of very long events (such as the loop state of the Q60G mutant) is more prone to uncertainties due to low signal-to-noise ratio of the TPM measurement. Similarly to what was discussed above for the measurements with wt-LacI at 4 pM, it should be noticed that the TPM measurements have a range of events durations which is optimal with respect to the diffusion time of the microsphere, the signal-to-noise ratio of the method and the mechanical stability of the experimental apparatus; as the limits of this range are approached, the measurements become subject to larger uncertainties. The range of validity of the TPM methodology is discussed in Supplementary Data. However, within experimental errors, the values of J_m and α measured for the Q60G mutant are not significantly different from those measured in the other experimental conditions. Thus, we can conclude that the point mutations studied (which are responsible for a variation of the flexibility of the hinge

region and, especially in the case of Q60 + 1, of the steric constraints of the protein head with respect to the core) lead to significant changes in the duration of the looped state, while not significantly affecting the sensitivity of this state to DNA strain. This observation has interesting implications with respect to the role of protein flexibility in the modulation of loop formation and disruption kinetics, as discussed in more detail below.

DISCUSSION

Due to its versatility and simplicity, the TPM method has been used for the study of a variety of biochemical systems at the single molecule level (20,24,25,33–36). With regard to dynamic measurements, the main limitation of this experimental approach is represented by the low signal-to-noise ratios that can be accomplished. This limitation is mostly determined by the size of the microspheres used, which defines the time necessary for the diffusive motion to explore the volume available for a certain tether length (see Figure 1); variations in the length of the tether can be detected on timescales longer than this characteristic diffusion time. This limitation may be overcome and much higher signal-to-noise ratios (or, equivalently, higher temporal resolution in the measurements) may be accomplished substituting much faster diffusing objects (such as quantum dots) for the microspheres thus far used. When implemented using microspheres, however, TPM requires care in the quantitative interpretation of the measured lifetimes. Figure 7, in fact, demonstrates how filtering of the experimental recordings (needed to obtain a good discrimination between the loop and unloop states) strongly influences the values of the measured lifetimes. We have elaborated a method of analysis of TPM data to overcome these problems and reliably measure the kinetic parameters of Lac repressor-induced loop formation and disruption.

The formation of the 305 bp long loop in our DNA construct by simultaneous binding of the Lac repressor tetramer to the two operators is associated with a bending energy in the DNA molecule corresponding to about 9.5 k_BT (37,38), calculated simplifying the loop geometry to a circle, and with a DNA persistence length of 50 nm (39,40). The spacing between operators in the Lac operon is 92 and 401 bp (4,5), thus the bending energies involved in the formation of these loops can be significant and may play an important role in the kinetics of transcription regulation. The effects of DNA tension and torsion on the kinetics of DNA-binding proteins have recently been explored in a variety of theoretical studies (13–15) and in experimental measurements on Gal repressor (41).

Single molecule approaches are providing fundamental information on the mechanical properties of a growing number of enzymatic systems *in vitro* (42). The measurement of forces in the pN range has indicated nucleic acid processing enzymes (such as RNA polymerase, DNA polymerase, topoisomerases) as molecular motors (43–45) capable of producing forces even larger than those of 'classic' motors, such as myosin (46) or kinesin (47,48). These forces may be crucial for these enzymes to overcome obstacles, unwind double-stranded structures and move along the DNA template under the conditions of compaction, tension and torsion to which it is subject *in vivo*. Transcription regulation systems, including the Lac operon, are sensitive to these forces to the extent by which binding and dissociation of the regulatory proteins are influenced by the bending and twisting energetics of the DNA. Measurements based on the use of magnetic tweezers have clearly demonstrated the sensitivity of the GalR system to supercoiling in the DNA target molecule (41). The persistence length of DNA *in vivo* is much lower than that measured *in vitro* (6), due to the action of accessory proteins. It is presumable that this physical property of DNA can be modulated to some extent by the quantity and quality of accessory proteins expressed in the cell. Thus, a new concept is recently emerging in gene regulation: the physical properties of DNA may play an important role in shaping the dynamics of gene regulation (38,49).

We have applied the TPM technique, in combination with a new method for data analysis, to the investigation of the effects of flexibility (both in DNA and in the hinge region of the protein) on the kinetics of loop formation and disruption.

The analysis of the kinetics of loop disruption is simplified by the fact that there is a 1:1 correspondence between the TPM state of lower microsphere mobility and the biochemical ORO state (see Figure 6). This correspondence is confirmed by the lack of dependence of τ_{Lm} on LacI concentration (Figure 4, left panels; Figure 7a, filled symbols). In fact, as an alternative interpretation, one could imagine a fast equilibrium between O-OR and ORO, characterized by rates much faster then the diffusion rate of the microsphere and shifted toward ORO, so to give raise to an apparent TPM loop state concealing fast biochemical reactions. However, if this were the case, one would expect the durations of the observed TPM loop state to depend on the concentration of LacI. In fact, the exit from the fast equilibrium would be determined by a reaction leading the system into a third, long lived, state. The most relevant long lived state in this regard depends on the concentration of LacI, and thus the entire behavior of the system is dependent on this parameter. More precisely, the ratio between the rates from O-OR toward RO-OR and O-O is given by $[LacI]/K_D$, which has a value of about 10, 2 and 0.4 for [LacI] of 100, 20 and 4 pM, respectively. At the two higher concentrations, RO-OR is, thus, prevalent: under these conditions, the rate of transition between O-OR and the other main unloop state scales linearly with [LacI]. Thus, the probability of exiting the above mentioned hypothetical equilibrium would also scale linearly with [LacI]. Since the measured duration of the TPM loop state does not depend on the concentration of LacI over a broad range of concentrations [4, 20 and 100 pM tested in this work, and 100 pM and 1 nM tested by Finzi and Gelles (20)] the hypothesis of the TPM loop state underlying a fast biochemical equilibrium is not likely; rather, the exit from this TPM state monitors directly the disruption of the loop in the DNA molecule. Thus, the TPM measurement provides a means for directly monitoring the effect of the loop strain on the kinetics of dissociation, as described in the results by the parameter α. Our findings indicate a weak dependence of the rate of loop disruption on the DNA bending and twisting energy, as demonstrated by the value of α between 1 and 2.

With regard to the kinetics of loop formation, on the other hand, our measurements indicate that formation of a loop in the DNA molecule by binding of Lac repressor simultaneously to two operators is highly sensitive to the DNA bending energy. Qualitatively, this result is well-expected based both on theoretical considerations and previous ligase-catalyzed circularization experiments; however, our results on LacI are somewhat surprising quantitatively. In fact, the values we have obtained for J_m (of the order of 10^{-10} M) are significantly lower than those measured by ligase-catalyzed cyclization experiments [$>10^{-8}$ M for DNA segments of 300 bp (8)] and calculated from physical models of the DNA molecule (11). It is fundamental to evaluate the effects of the microsphere on the values measured for J_m by TPM technique. It is expected, in fact, that the presence of the microsphere may slow down the kinetics of loop formation, due to an effective swelling force exerted entropically by the microsphere on the polymer. Below we will discuss results indicating that, in a system like the one we setup for the measurements on LacI, the effect of the microsphere on the measured kinetics of loop formation (and, therefore, on the measured J_m) should not exceed, at most, a factor of 10.

In their theoretical work, extensively modeling the physical properties of the TPM system, Segall *et al*. provide an analytical expression [Equation 12 in Ref. (50)] for the swelling force as a function of DNA contour length, persistence length and microsphere radius. In our experimental system, the swelling force estimated according to this expression is about 30 fN. Segall *et al*. (50) conclude that a force of this magnitude due to the presence of the microsphere would decrease the rate of looping by about a factor of 2.

Further, the TPM recordings of the position distributions of the microsphere in the absence of Lac repressor exhibit interesting non-Gaussian features (25) which may be exploited to estimate the magnitude of the swelling force. Using numerical simulations of the TPM system [similar to those described by Segall *et al*. (50)] to fit our data, we have estimated in our system an effective swelling force of 127 ± 14 fN (best estimate ± range for 95.4% confidence; see Supplementary Data). Recent theoretical works (14,51) have described the effects of force on J_m: a force in the range between 30 and 140 fN due to the presence of the microsphere would not be expected to decrease J_m by more than a factor of 10.

Finally, Hsieh *et al*. (19) reported an estimate of the equilibrium constant K^* for the intramolecular looping reaction: for the pRW490 construct containing the two primary operators at a distance of 305 bp from each other, they reported a value of 16 for K^*. In our measurements, the equilibrium constant for the intramolecular looping reaction is given by $K' = J_m k_a / (2k_d\alpha)$. Using the values of J_m and α reported in Table 1 we obtain K' between 2.5 and 7. The difference between K^* and K' is to be attributed to the microsphere, according to the following relationship: $-RT \ln(K') = \Delta G_{tpm} = \Delta G_{DNA/LacI} + \Delta G_{bead}$, where $\Delta G_{DNA/LacI} = -RT \ln(K^*)$ is the free energy of looping in the absence of microsphere and ΔG_{bead} is the positive free energy contribution due to the microsphere opposing an entropic force to the formation of the loop. From these relations, based on the measurement of K' reported above, we estimate ΔG_{bead} between 0.8 and 1.8 k_BT. If we assume that this energetic barrier affects mostly the rate of formation of the loop, this would lead to a reduction of the looping rate by at most 55–83%, in agreement with what calculated by Segall *et al*. (50). Thus, we conclude that, even accounting for an underestimation of J_m by about an order of magnitude in TPM due to the microsphere, Lac repressor looping is characterized by a J_m much (at least 10 times) lower than the ligase-catalyzed circularization of a DNA segment of the same length.

The shape of a DNA loop can vary over a wide range of geometries determining large variations in the loop energetics and in the resulting J_m values (15,49), with significant deviations from those measured in cyclization experiments. Also, the effect of the protein bridging between the two extremities of the loop significantly influences the calculated values of J_m (52,53).

The structure of the DNA–LacI complex in the looped configuration has not yet been determined. In addition to the original V-shaped model, proposed by Lewis *et al*. (54), an extended conformation of the Lac repressor has been proposed (55). The rigidity of these conformations and the possibility for the protein to switch between these multiple structural states are fundamental in determining J_m for loop formation. Also, distance and phasing between the operators is a fundamental factor in determining the value of J_m, as already demonstrated for ligase-catalyzed circularization. The TPM method holds promise to allow a systematic characterization of the dependence of LacI regulation of the Lac operon on each of these components, providing in the near future, a complete picture of the orientation effects and of the protein and DNA mechanics involved in the process.

Our measurements on the mutants of the hinge region Q60G and Q60 + 1 indicate that alterations in the flexibility and geometry of the hinge lead to significant changes in the kinetics measurable with TPM. The association and dissociation rate constants for these mutants have not been measured in standard biochemical assays; however, the data shown in Figure 7b clearly demonstrate the large effects of these mutations on the looped lifetimes, with much smaller effects on the unlooped lifetimes. These results lead to the conclusion that the mutations studied cause changes predominantly in the value of the dissociation rate constant. As expected, the mutant characterized by the lower equilibrium dissociation constant (Q60G) displays a longer looped average lifetime, whereas the mutant with the higher K_D (Q60 + 1) displays a shorter looped average lifetime. However, the sensitivity of the protein to DNA strain is not significantly affected by these mutations. It is likely that a role of this kind may be more appropriate for the tetramerization domain, and for the regions of interaction between monomers in the tetramer, which affect the propensity of the protein to take a V-shape, an open shape or other possible conformations responsible for a different sensitivity to strain in the DNA target.

In conclusion, with regard to DNA bending, our work indicates that the rate of loop formation by Lac repressor depends more strongly than previously expected on the energetics of bending and twisting of DNA. Therefore, the mechanical and biochemical factors that *in vivo* modulate

these energetics can play a crucial role in the modulation of gene expression regulation at least in the paradigmatic example of the Lac operon. With regard to the protein flexibility, on the other hand, our results show that the hinge flexibility and geometry have a determinant effect especially on the lifetime of the looped state, demonstrating the interplay of the mechanical properties of partners in this classic example of protein–DNA interacting system.

Future steps aimed at a further characterization of the TPM system will investigate the effect of microspheres of different sizes on TPM measurements. Also, the measurement of looping and unlooping kinetics of different constructs in which the distances and phasing between operators is varied will provide important additional information.

SUPPLEMENTARY DATA

Supplementary Data are available at NAR online.

ACKNOWLEDGEMENTS

A special acknowledgement goes to Dr Giovanni Romano for his preliminary work. We are grateful to Drs Kathleen S. Matthews and Hongli Zhan (Rice University) for stimulating discussions and for the generous gift of the plasmids for DNA and protein expression. We thank Drs Davide Normanno and Marco Capitanio (LENS) for discussions and useful comments during the experiments and the writing of the manuscript. This work was supported by the European Union Contract RII3-CT-2003-506 350. L.S. is grateful to the Ente Cassa di Risparmio di Firenze for financial support. Funding to pay the Open Access publication charges for this article was provided by LENS.

Conflict of interest statement. None declared.

REFERENCES

1. Jacob,F. and Monod,J. (1961) Genetic regulatory mechanisms in the synthesis of proteins. *J. Mol. Biol.*, **3**, 318–356.
2. Lewis,M. (2005) The lac repressor. *C. R. Biol.*, **328**, 521–548.
3. Matthews,K.S. (1992) DNA looping. *Microbiol. Rev.*, **56**, 123–136.
4. Reznikoff,W.S., Winter,R.B. and Hurley,C.K. (1974) The location of the repressor binding sites in the lac operon. *Proc. Natl Acad. Sci. USA*, **71**, 2314–2318.
5. Pfahl,M., Gulde,V. and Bourgeois,S. (1979) 'Second' and 'third operator' of the lac operon: an investigation of their role in the regulatory mechanism. *J. Mol. Biol.*, **127**, 339–344.
6. Ringrose,L., Chabanis,S., Angrand,P.O., Woodroofe,C. and Stewart,A.F. (1999) Quantitative comparison of DNA looping *in vitro* and *in vivo*: chromatin increases effective DNA flexibility at short distances. *EMBO J.*, **18**, 6630–6641.
7. Shore,D., Langowski,J. and Baldwin,R.L. (1981) DNA flexibility studied by covalent closure of short fragments into circles. *Proc. Natl Acad. Sci. USA*, **78**, 4833–4837.
8. Shore,D. and Baldwin,R.L. (1983) Energetics of DNA twisting. I. Relation between twist and cyclization probability. *J. Mol. Biol.*, **170**, 957–981.
9. Cloutier,T.E. and Widom,J. (2005) DNA twisting flexibility and the formation of sharply looped protein–DNA complexes. *Proc. Natl Acad. Sci. USA*, **102**, 3645–3650.
10. Du,Q., Smith,C., Shiffeldrim,N., Vologodskaia,M. and Vologodskii,A. (2005) Cyclization of short DNA fragments and bending fluctuations of the double helix. *Proc. Natl Acad. Sci. USA*, **102**, 5397–5402.
11. Shimada,J. and Yamakawa,H. (1984) Ring-closure probabilities for twisted wormlike chains. Application to DNA. *Macromolecules*, **17**, 689–698.
12. Rippe,K., von Hippel,P.H. and Langowski,J. (1995) Action at a distance: DNA-looping and initiation of transcription. *Trends Biochem. Sci.*, **20**, 500–506.
13. Marko,J.F. and Siggia,E.D. (1997) Driving proteins off DNA using applied tension. *Biophys. J.*, **73**, 2173–2178.
14. Blumberg,S., Tkachenko,A.V. and Meiners,J.C. (2005) Disruption of protein-mediated DNA looping by tension in the substrate DNA. *Biophys. J.*, **88**, 1692–1701.
15. Sankararaman,S. and Marko,J.F. (2005) Formation of loops in DNA under tension. *Phys. Rev. E Stat. Nonlin. Soft Matter Phys.*, **71**, 021911.
16. Kramer,H., Niemoller,M., Amouyal,M., Revet,B., von Wilcken-Bergmann,B. and Muller-Hill,B. (1987) lac repressor forms loops with linear DNA carrying two suitably spaced lac operators. *EMBO J.*, **6**, 1481–1491.
17. Mossing,M.C. and Record,M.T.,Jr (1986) Upstream operators enhance repression of the lac promoter. *Science*, **233**, 889–892.
18. Muller,J., Oehler,S. and Muller-Hill,B. (1996) Repression of lac promoter as a function of distance, phase and quality of an auxiliary lac operator. *J. Mol. Biol.*, **257**, 21–29.
19. Hsieh,W.T., Whitson,P.A., Matthews,K.S. and Wells,R.D. (1987) Influence of sequence and distance between two operators on interaction with the lac repressor. *J. Biol. Chem.*, **262**, 14583–14591.
20. Finzi,L. and Gelles,J. (1995) Measurement of lactose repressor-mediated loop formation and breakdown in single DNA molecules. *Science*, **267**, 378–380.
21. Falcon,C.M. and Matthews,K.S. (1999) Glycine insertion in the hinge region of lactose repressor protein alters DNA binding. *J. Biol. Chem.*, **274**, 30849–30857.
22. Wycuff,D.R. and Matthews,K.S. (2000) Generation of an AraC-araBAD promoter-regulated T7 expression system. *Anal. Biochem.*, **277**, 67–73.
23. Chen,J. and Matthews,K.S. (1992) Deletion of lactose repressor carboxyl-terminal domain affects tetramer formation. *J. Biol. Chem.*, **267**, 13843–13850.
24. Vanzi,F., Vladimirov,S., Knudsen,C.R., Goldman,Y.E. and Cooperman,B.S. (2003) Protein synthesis by single ribosomes. *RNA*, **9**, 1174–1179.
25. Pouget,N., Dennis,C., Turlan,C., Grigoriev,M., Chandler,M. and Salome,L. (2004) Single-particle tracking for DNA tether length monitoring. *Nucleic Acids Res.*, **32**, e73.
26. Blumberg,S., Gajraj,A., Pennington,M.W. and Meiners,J.C. (2005) Three-dimensional characterization of tethered microspheres by total internal reflection fluorescence microscopy. *Biophys. J.*, **89**, 1272–1281.
27. Colquhoun,D. and Sigworth,F.J. (1983) Fitting and statistical analysis of single-channel records. In Sakmann,B. and Neher,E. (eds), *Single-Channel Recording*. Plenum Press, NY, pp. 191–263.
28. Colquhoun,D. and Sakmann,B. (1981) Fluctuations in the microsecond time range of the current through single acetylcholine receptor ion channels. *Nature*, **294**, 464–466.
29. Brenowitz,M., Pickar,A. and Jamison,E. (1991) Stability of a Lac repressor mediated 'looped complex'. *Biochemistry*, **30**, 5986–5998.
30. Levandoski,M.M., Tsodikov,O.V., Frank,D.E., Melcher,S.E., Saecker,R.M. and Record,M.T.,Jr (1996) Cooperative and anticooperative effects in binding of the first and second plasmid Osym operators to a LacI tetramer: evidence for contributions of non-operator DNA binding by wrapping and looping. *J. Mol. Biol.*, **260**, 697–717.
31. Barry,J.K. and Matthews,K.S. (1999) Thermodynamic analysis of unfolding and dissociation in lactose repressor protein. *Biochemistry*, **38**, 6520–6528.
32. Jacobson,H. and Stockmayer,W.H. (1950) Intramolecular reaction in polycondensations. I. The theory of linear systems. *J. Chem. Phys.*, **18**, 1600–1606.
33. Schafer,D.A., Gelles,J., Sheetz,M.P. and Landick,R. (1991) Transcription by single molecules of RNA polymerase observed by light microscopy. *Nature*, **352**, 444–448.
34. Yin,H., Landick,R. and Gelles,J. (1994) Tethered particle motion method for studying transcript elongation by a single RNA polymerase molecule. *Biophys. J.*, **67**, 2468–2478.
35. Tolic-Norrelykke,S.F., Engh,A.M., Landick,R. and Gelles,J. (2004) Diversity in the rates of transcript elongation by single RNA polymerase molecules. *J. Biol. Chem.*, **279**, 3292–3299.

36. van den Broek,B., Vanzi,F., Normanno,D., Pavone,F.S. and Wuite,G.J. (2006) Real-time observation of DNA looping dynamics of Type IIE restriction enzymes NaeI and NarI. *Nucleic Acids Res.*, **34**, 167–174.
37. Marko,J.F. and Cocco,S. (2003) The micromechanics of DNA. *Phys. World*, **16**, 37–41.
38. Saiz,L., Rubi,J.M. and Vilar,J.M. (2005) Inferring the *in vivo* looping properties of DNA. *Proc. Natl Acad. Sci. USA*, **102**, 17642–17645.
39. Hagerman,P.J. (1988) Flexibility of DNA. *Annu. Rev. Biophys. Biophys. Chem.*, **17**, 265–286.
40. Smith,S.B., Cui,Y. and Bustamante,C. (1996) Overstretching B-DNA: the elastic response of individual double-stranded and single-stranded DNA molecules. *Science*, **271**, 795–799.
41. Lia,G., Bensimon,D., Croquette,V., Allemand,J.F., Dunlap,D., Lewis,D.E., Adhya,S. and Finzi,L. (2003) Supercoiling and denaturation in Gal repressor/heat unstable nucleoid protein (HU)-mediated DNA looping. *Proc. Natl Acad. Sci. USA*, **100**, 11373–11377.
42. Capitanio,M., Vanzi,F., Broggio,C., Cicchi,R., Normanno,D., Romano,G., Sacconi,L. and Pavone,F.S. (2004) Exploring molecular motors and switches at the single-molecule level. *Microsc. Res. Tech.*, **65**, 194–204.
43. Yin,H., Wang,M.D., Svoboda,K., Landick,R., Block,S.M. and Gelles,J. (1995) Transcription against an applied force. *Science*, **270**, 1653–1657.
44. Strick,T.R., Croquette,V. and Bensimon,D. (2000) Single-molecule analysis of DNA uncoiling by a type II topoisomerase. *Nature*, **404**, 901–904.
45. Wuite,G.J., Smith,S.B., Young,M., Keller,D. and Bustamante,C. (2000) Single-molecule studies of the effect of template tension on T7 DNA polymerase activity. *Nature*, **404**, 103–106.
46. Finer,J.T., Simmons,R.M. and Spudich,J.A. (1994) Single myosin molecule mechanics: piconewton forces and nanometre steps. *Nature*, **368**, 113–119.
47. Ashkin,A., Schutze,K., Dziedzic,J.M., Euteneuer,U. and Schliwa,M. (1990) Force generation of organelle transport measured *in vivo* by an infrared laser trap. *Nature*, **348**, 346–348.
48. Svoboda,K. and Block,S.M. (1994) Force and velocity measured for single kinesin molecules. *Cell*, **77**, 773–784.
49. Zhang,Y., McEwen,A.E., Crothers,D.M. and Levene,S.D. (2006) Statistical-mechanical theory of DNA looping. *Biophys. J.*, **90**, 1903–1912.
50. Segall,D.E., Nelson,P.C. and Phillips,R. (2006) Volume-exclusion effects in tethered-particle experiments: bead size matters. *Phys. Rev. Lett.*, **96**, 088306.
51. Yan,J., Kawamura,R. and Marko,J.F. (2005) Statistics of loop formation along double helix DNAs. *Phys. Rev. E Stat. Nonlin. Soft Matter Phys.*, **71**, 061905.
52. Merlitz,H., Rippe,K., Klenin,K.V. and Langowski,J. (1998) Looping dynamics of linear DNA molecules and the effect of DNA curvature: a study by Brownian dynamics simulation. *Biophys. J.*, **74**, 773–779.
53. Rippe,K. (2001) Making contacts on a nucleic acid polymer. *Trends Biochem. Sci.*, **26**, 733–740.
54. Lewis,M., Chang,G., Horton,N.C., Kercher,M.A., Pace,H.C., Schumacher,M.A., Brennan,R.G. and Lu,P. (1996) Crystal structure of the lactose operon repressor and its complexes with DNA and inducer. *Science*, **271**, 1247–1254.
55. Edelman,L.M., Cheong,R. and Kahn,J.D. (2003) Fluorescence resonance energy transfer over approximately 130 base pairs in hyperstable lac repressor-DNA loops. *Biophys. J.*, **84**, 1131–1145.